Accelerated Publications

The C_2B Domain of Synaptotagmin I Is a Ca^{2+}-Binding Module†

Josep Ubach,[‡,§] Ye Lao,[||,⊥,#] Imma Fernandez,[‡,§] Demet Arac,[‡,§] Thomas C. Südhof,[||,⊥,#] and Josep Rizo*[,‡,§]

Departments of Biochemistry, Pharmacology, and Molecular Genetics, Center for Basic Neuroscience, and Howard Hughes Medical Institute, University of Texas Southwestern Medical Center, 5323 Harry Hines Boulevard, Dallas, Texas 75390

Received February 16, 2001; Revised Manuscript Received April 2, 2001

ABSTRACT: Synaptotagmin I is a synaptic vesicle protein that contains two C_2 domains and acts as a Ca^{2+} sensor in neurotransmitter release. The Ca^{2+}-binding properties of the synaptotagmin I C_2A domain have been well characterized, but those of the C_2B domain are unclear. The C_2B domain was previously found to pull down synaptotagmin I from brain homogenates in a Ca^{2+}-dependent manner, leading to an attractive model whereby Ca^{2+}-dependent multimerization of synaptotagmin I via the C_2B domain participates in fusion pore formation. However, contradictory results have been described in studies of Ca^{2+}-dependent C_2B domain dimerization, as well as in analyses of other C_2B domain interactions. To shed light on these issues, the C_2B domain has now been studied using biophysical techniques. The recombinant C_2B domain expressed as a GST fusion protein and isolated by affinity chromatography contains tightly bound bacterial contaminants despite being electrophoretically pure. The contaminants bind to a polybasic sequence that has been previously implicated in several C_2B domain interactions, including Ca^{2+}-dependent dimerization. NMR experiments show that the pure recombinant C_2B domain binds Ca^{2+} directly but does not dimerize upon Ca^{2+} binding. In contrast, a cytoplasmic fragment of native synaptotagmin I from brain homogenates, which includes the C_2A and C_2B domains, participates in a high molecular weight complex as a function of Ca^{2+}. These results show that the recombinant C_2B domain of synaptotagmin I is a monomeric, autonomously folded Ca^{2+}-binding module and suggest that a potential function of synaptotagmin I multimerization in fusion pore formation does not involve a direct interaction between C_2B domains or requires a posttranslational modification.

Synaptotagmins constitute a large family of neuronal membrane proteins (*1*, *2*). Synaptotagmin I, the first member identified in this family, is a synaptic vesicle protein that is essential for fast Ca^{2+}-triggered neurotransmitter release (*3*), most likely acting as a Ca^{2+} sensor in this process (*4*, *5*). Synaptotagmin I contains an N-terminal intravesicular sequence, a transmembrane region, a linker sequence, and two C-terminal C_2 domains referred to as the C_2A and C_2B domains (Figure 1A). The synaptotagmin I C_2A domain has a β-sandwich structure and binds multiple Ca^{2+} ions via a motif that includes five conserved aspartate residues at the tip of the β-sandwich (*6*−*8*). The C_2B domain from the Rab3 effector protein rabphilin, which shares substantial sequence homology with the synaptotagmin I C_2B domain (Figure 1B), also forms a β-sandwich structure (see Figure 1C) and binds multiple Ca^{2+} ions via a similar motif (*9*). On the basis of this homology and its Ca^{2+}-dependent activities (see below), it has been hypothesized that the synaptotagmin I C_2B domain also binds Ca^{2+} and contributes to the Ca^{2+}-sensing function of synaptotagmin I, but this hypothesis has not been directly tested. In addition, while both C_2 domains of synaptotagmin I have been implicated in several interactions that could mediate its function in neurotransmitter release (reviewed in refs 1 and 2), the interactions involving the C_2B domain have been controversial.

Particular attention has attracted the involvement of the C_2B domain in Ca^{2+}-dependent synaptotagmin multimerization. Since synaptotagmin I forms Ca^{2+}-independent constitutive dimers via its transmembrane region (*10*−*13*), the observation that the recombinant C_2B domain immobilized as a GST[1] fusion captured native synaptotagmin I from brain extracts in a Ca^{2+}-dependent manner (*14*, *15*) led to an attractive model whereby Ca^{2+}-dependent self-association could result in a ring of synaptotagmins during fusion pore formation. Moreover, the observation that different synap-

† This work was supported by a grant from the Welch Foundation and by NIH Grant NS40944.

* To whom correspondence should be addressed. Tel: 214-648-9026. Fax: 214-648-8673. E-mail: jose@arnie.swmed.edu.

‡ Department of Biochemistry.

§ Department of Pharmacology.

|| Department of Molecular Genetics.

⊥ Center for Basic Neuroscience.

Howard Hughes Medical Institute.

[1] Abbreviations: ES-MS, electrospray−mass spectrometry; GST, glutathione *S*-transferase; HSQC, heteronuclear single-quantum correlation; SNAP, soluble NSF attachment protein; SNARE, SNAP receptor; SV2, synaptic vesicle protein 2.

10.1021/bi010340c CCC: $20.00
Published on Web 04/25/2001

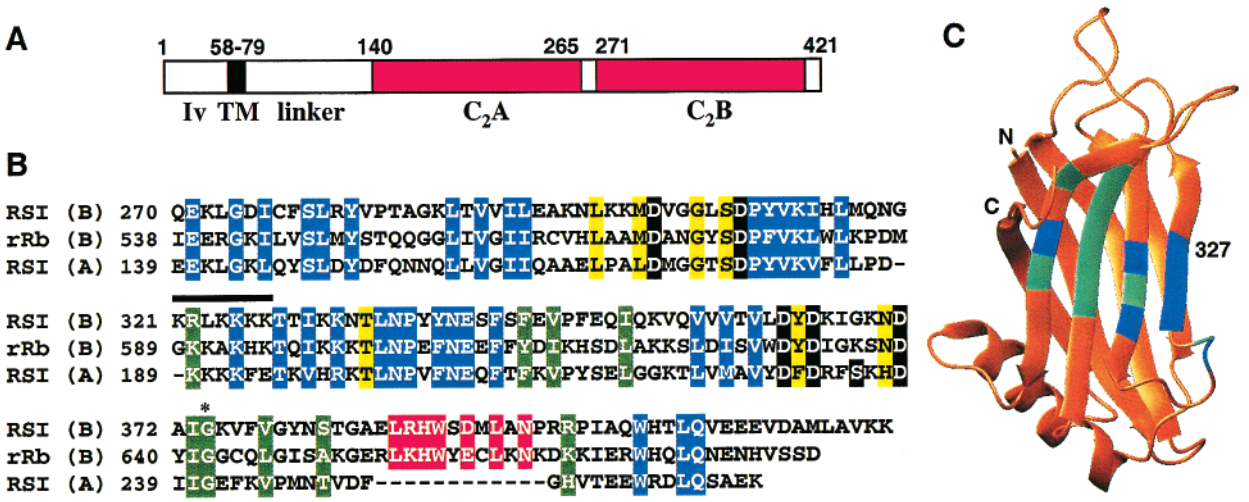

FIGURE 1: Domain diagram of synaptotagmin I and structural model of its C_2B domain. (A) Domain diagram with the different regions of the synaptotagmin I sequence indicated below (Iv, intravesicular sequence; TM, transmembrane region) and their approximate boundaries indicated above. The two C_2 domains are represented by red boxes. (B) Sequence alignment of the rat synaptotagmin I (RSI) C_2A and C_2B domains and the rat rabphilin (rRb) C_2B domain. Residues involved in Ca^{2+} binding to the synaptotagmin I C_2A domain (*8*) and the rabphilin C_2B domain (*9*), as well as those predicted to bind Ca^{2+} in the synaptotagmin I C_2B domain based on the observed homology, are shown with a dark background. Other background color coding highlights conserved residues according to their location in the three-dimensional structures of C_2 domains, which consist of a β-sandwich with loops emerging at the top and the bottom (*6*−*9*): blue, β-strands; yellow, top loops; green, bottom loops. A specific feature of C_2B domains, not present in C_2A domains, is an α-helix at the bottom of the domain (conserved residues highlighted in red) (*9*). Gly374 of the synaptotagmin I C_2B domain, which was an aspartate in the original rat sequence, is indicated with an asterisk, and the polybasic region is indicated by a solid bar. (C) Ribbon diagram of the structure of the rabphilin C_2B domain (*9*) that we use as a model for the structure of the synaptotagmin I C_2B domain. The positions of residues exhibiting $^1H-^{15}N$ HSQC cross-peak shifts due to binding of contaminants to the synaptotagmin I C_2B domain (see Figure 5) are colored in blue (for basic residues) or cyan (for other residues). The position of K327 is labeled to indicate the location of strand 4, which contains the polybasic sequence involved in binding to the contaminants. N- and C-termini are indicated by N and C, respectively. The ribbon diagram was prepared with the program Molmol (*39*).

totagmin isoforms can form heterodimers (*16*−*22*) has led to models whereby heterooligomerization of different combinations of synaptotagmins may lead to Ca^{2+} sensors with distinct Ca^{2+} sensitivities, although at least some of these combinations may not be relevant since not all synaptotagmins are localized on synaptic vesicles (*23*). Furthermore, it is unclear whether the synaptotagmin I C_2B domain actually dimerizes as a function of Ca^{2+}. Thus, direct Ca^{2+}-dependent dimerization of the recombinant C_2B domain and the double C_2 domain region has been reported in one study (*21*) but disputed in another (*24*).

The significance of other interactions described for the synaptotagmin I C_2B domain is also unclear. The C2B domain was found to bind in a Ca^{2+}-independent manner to the clathrin adaptor protein AP-2 (*25*), Ca^{2+} channels (*26*), and inositol polyphosphates (*27*). However, all of these interactions were found to involve the same site of the C_2B domain, a polybasic region that was also implicated in dimerization, and some of them can be reproduced with incomplete C_2B domain fragments (*16*, *28*) that are unlikely to be properly folded. In addition, interactions of the C_2B domain with β-SNAP and with SV2 were observed in some studies (*29*, *30*) but not in others (*16*, *21*). It is possible that these contradictory results may have arisen in part from the common use of immobilized GST−C_2B domain fusions that are isolated by affinity chromatography without further purification.

In view of the central function of synaptotagmin I in Ca^{2+}-triggered exocytosis and the potential importance of Ca^{2+}-dependent synaptotagmin multimerization, we have now investigated whether the C_2B domain is in fact a Ca^{2+}-binding module and whether it dimerizes as a function of Ca^{2+}. We find that GST−C_2B domain fusion proteins produced by standard approaches are highly contaminated by nonproteinaceous impurities. We have developed a procedure to obtain a properly folded, pure C_2B domain and show that the C_2B domain does bind Ca^{2+} but remains monomeric upon Ca^{2+} binding. These results suggest that the C_2B domain cooperates with the C_2A domain in the Ca^{2+} sensor function of synaptotagmin I via Ca^{2+}-dependent interactions with target molecules other than the C_2B domain itself.

EXPERIMENTAL PROCEDURES

Protein Expression, Purification, and Spectroscopy. Since with an Asp374→Gly substitution the amino acid sequence of the rat synaptotagmin I C_2 domains is identical to the bovine sequence, DNA fragments encoding the rat C_2B domain (residues 271−421) and double C_2 domain region (residues 140−421) were obtained by PCR amplification from bovine synaptotagmin I cDNA using customary designed primers (we use the rat sequence numbers to avoid confusions in the literature). The PCR products were subcloned into the pGEX-KG vector (*31*) and expressed in *Escherichia coli* BL21 using LB medium or minimal medium containing $^{15}NH_4Cl$ as the sole nitrogen source for ^{15}N-labeling. Cell pellets were resuspended in PBS, passed three times through an EmulsiFlex-C5 cell disrupter (Avestin) at 14 000 psi and spun at 28000*g* for 30 min. The supernatants were then incubated with glutathione−agarose (1 mL/L of culture). For standard preparations, the resin was extensively washed with PBS until there was no detectable UV absorption in the eluate, equilibrated with cleavage buffer (50 mM Tris, pH 8.0, 0.2 M NaCl, 2.5 mM $CaCl_2$), and cleaved with

thrombin (1.8 NIH units/mL) at 25 °C for 1.5 h. For optimal purification of the C_2B domain, the resin was extensively washed with 50 mM $CaCl_2$ in cleavage buffer after the PBS wash and prior to the cleavage step, and the cleaved products were purified by gel filtration on Superdex 75 (Pharmacia) (0.2 M phosphate, pH 6.3, 0.3 M NaCl) followed by cation-exchange chromatography on SourceS (Pharmacia) in 20 mM MES, pH 6.3, and 20 mM $CaCl_2$ using a linear gradient from 0.3 to 0.6 M NaCl in 8 column volumes. The elevated salt concentration was critical to obtain good resolution by gel filtration since the C_2B domain is highly basic and binding to the slightly negatively charged solid matrix at lower salt results in partial retention of the protein in the column (see Figure 2B). UV spectra were acquired on a Hewlett-Packard 8452A spectrophometer. NMR spectra were acquired on a Varian INOVA600 under the conditions described in the legends of Figures 3−5. $^1H-^{15}N$ HSQC spectra were acquired using a sensitivity-enhanced pulse sequence (*32*) with total acquisition times of 1−2 h.

Gel Filtration of Native Synaptotagmin I. Four frozen rat brains were homogeneized in 16 mL of 20 mM HEPES, pH 7.4, 0.1 M NaCl, 0.1 g/L PMSF, 10 mg/L leupeptin, 10 mg/L aprotinin, and 1 mg/L pepstatin, in the presence of 2.5 mM $CaCl_2$, 2.5 mM $MgCl_2$, or 2.5 mM EGTA as indicated. The homogenate was treated with 0.008% trypsin at 37 °C for 30 min, and the proteolysis was terminated with 0.1 g/L soybean trypsin inhibitor, 1% goat serum, and 1 g/L PMSF. Insoluble material was removed by centrifugation for 15 min at 2 °C, 80 000 rpm. Gel filtration of 2 mL samples was performed on Superdex 75 with 20 mM HEPES (pH 7.4) and 0.1 M NaCl, and 3 mL fractions precipitated with trichloroacetic acid were analyzed by SDS−PAGE followed by immunoblotting.

RESULTS

Preparation of the Pure, Properly Folded C_2B Domain. To characterize the C_2B domain structurally and functionally, it is necessary to obtain pure and properly folded recombinant protein, but two significant problems hindered such characterizarion. First, we noticed that our original rat synaptotagmin I sequence contained an aspartate residue at position 374 (*33*) while our sequences of human, bovine, mouse, and *Drosophila* synaptotagmin I (*3*, *10*, *34*, *35*), as well as a more recently cloned rat sequence (*17*), contained a glycine at the same position. These observations suggested the possibility of a cloning artifact in the original rat cDNA clones, although another recent study found that both aspartate and glycine residues were present at position 374 in PCR products using rat cDNA as a template (*21*). Extensive attempts to prepare the C_2B domain with the original sequence as a GST fusion or with a His_6 tag yielded electrophoretically pure proteins, but they were largely unfolded (data not shown). The folding problem was circumvented by expression of the recombinant C_2B domain with a glycine at position 374, which was therefore used in all subsequent studies. These results, and the fact that this glycine residue is highly conserved not only in synaptotagmins but also in C_2 domains in general (see sequence alignment in ref *36*), suggest that this glycine is critical for the C_2 domain fold and that the presence of an aspartate in this position in the original rat synaptotagmin I sequence was indeed artifactual.

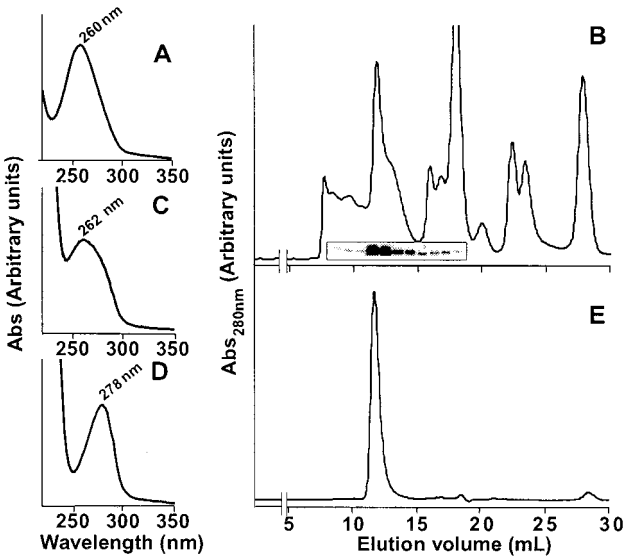

FIGURE 2: The C_2B domain obtained by standard GST fusion methodology is highly impure. (A) UV spectrum of the C_2B domain obtained after thrombin cleavage of a GST−C_2B domain fusion purified by standard affinity chromatography on glutathione−agarose. (B) Gel filtration of the same sample on Superdex 75 in 20 mM MES, pH 6.3, and 0.2 M NaCl. Coomassie Blue-stained C_2B domain bands from SDS−PAGE of the eluted fractions are indicated below the chromatographic profile. (C) UV spectrum of the major C_2B domain fraction from the chromatogram shown in (B). (D) UV spectrum of the C_2B domain purified by the optimal procedure described in the text. (E) Gel filtration of the same purified sample on Superdex 75 in 20 mM MES buffer, pH 6.3, and 0.4 M NaCl.

The second problem we encountered was related to the purification of the C_2B domain with the correct Gly374 sequence. Expression of the C_2B domain as a GST fusion, and isolation by affinity chromatography on glutathione−agarose using standard procedures, yielded a fusion protein that appeared to be highly pure by SDS−PAGE. However, the UV spectrum of the isolated C_2B domain obtained after on-resin thrombin cleavage exhibited a maximum at 260 nm uncharacteristic of polypeptides (Figure 2A). Furthermore, gel filtration chromatography (Figure 2B) revealed the presence of numerous nonprotein contaminants, most of them with absorption maxima at 260 nm. In fact, the fractions containing most of the C_2B domain still had strong absorption at 260 nm (Figure 2C). Although the chromatographic profiles varied substantially in different preparations, large amounts of contaminants were observed in all cases, even when the cell supernatant was treated with DNase or polyethylenimine or when the immobilized fusion protein was extensively washed with 1 M NaCl. The contaminants were heterogeneous, and their nature could not be completely established, but ^1H NMR spectra revealed the presence of small oligonucleotides (data not shown).

To eliminate the bacterial contaminants, we developed a purification procedure that includes extensive washes of the resin-immobilized GST−C_2B domain fusion with 50 mM Ca^{2+} as a key step to reduce the UV absorption at 260 nm of the thrombin-cleaved material. After gel filtration at high ionic strength and cation-exchange chromatography in the presence of 20 mM Ca^{2+}, the purified material had a UV absorption maximum at 278 nm (Figure 2D) and eluted as a single peak in gel filtration (Figure 2E). ES-MS revealed a single species with the expected molecular weight. The high

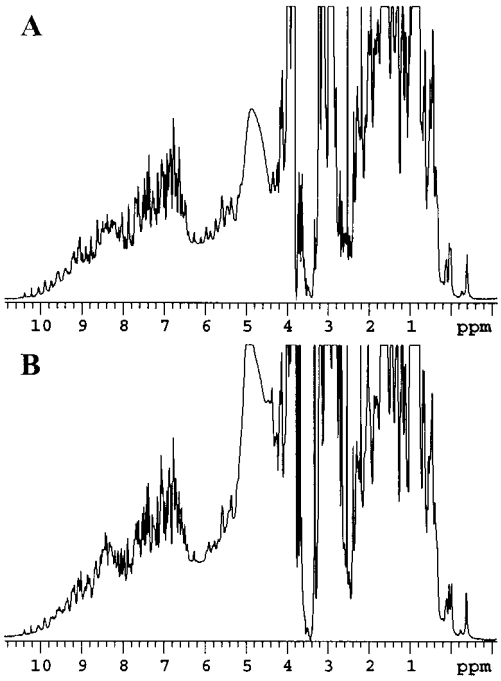

FIGURE 3: ^{1}H NMR spectra of the C_2B domain show that it is well folded and monomeric in the absence and presence of Ca^{2+}. The spectra were acquired at 600 MHz and 30 °C in 50 mM MES (pH 6.3), 0.15 M NaCl, and 2 mM DTT, with samples containing 1.1 mM C_2B domain and 20 mM Ca^{2+} (A) or 0.4 mM C_2B domain and 1 mM EDTA (B). The spectra are displayed at high vertical scale to emphasize the resonances in well-resolved regions of the spectra.

quality and excellent chemical shift dispersion observed in the NMR spectra of the pure C_2B domain (Figures 3 and 4A) suggest that it is a well-folded protein module with the characteristic β-sandwich structure found in other C_2 domains (*6*, *9*). Complete resonance assignments of the C_2B domain, which are currently being used to solve its three-dimensional structure, confirm this conclusion.[2]

The C_2B Domain Binds Ca^{2+} but Does Not Dimerize. Comparison of the ^{1}H−^{15}N HSQC spectra of the C_2B domain obtained in the absence and presence of Ca^{2+} (Figure 4A) revealed substantial Ca^{2+}-induced shifts in a subset of cross-peaks, showing that the isolated C_2B domain binds Ca^{2+} directly. Major Ca^{2+}-induced shifts were only observed for residues in the loops that are predicted to bind Ca^{2+} at the top of the β-sandwich, as observed for other C_2 domains (*9*, *37*). The Ca^{2+} dependence of the cross-peak shifts, illustrated for a representative cross-peak in Figure 4B,C, indicates an intrinsic Ca^{2+} affinity of ca. 500 μM. Note that the synaptotagmin I C_2A domain also has a low intrinsic Ca^{2+} affinity that arises from incomplete coordination of the Ca^{2+} ions (*8*), but this affinity increases considerably in Ca^{2+}-dependent binding to ternary components that may complete the Ca^{2+} coordination spheres (e.g., phospholipids; see ref *38*). Hence, our NMR results show that the isolated C_2B domain of synaptotagmin I is a functional Ca^{2+}-binding domain with intrinsic Ca^{2+}-binding properties similar to those of the C_2A domain.[2]

Since dimerization of globular proteins is expected to substantially increase the line widths of their resonances due to the increase in effective molecular weight, we examined whether Ca^{2+} causes resonance broadening in the ^{1}H NMR spectrum of the C_2B domain (Figure 3). Surprisingly, the resonances were slightly broader in the absence of Ca^{2+}, probably because the Ca^{2+}-free C_2B domain has a higher tendency to aggregate and cannot be concentrated to more than 0.4 mM under our experimental conditions. In contrast, the C_2B domain can be concentrated to 1.3 mM in the

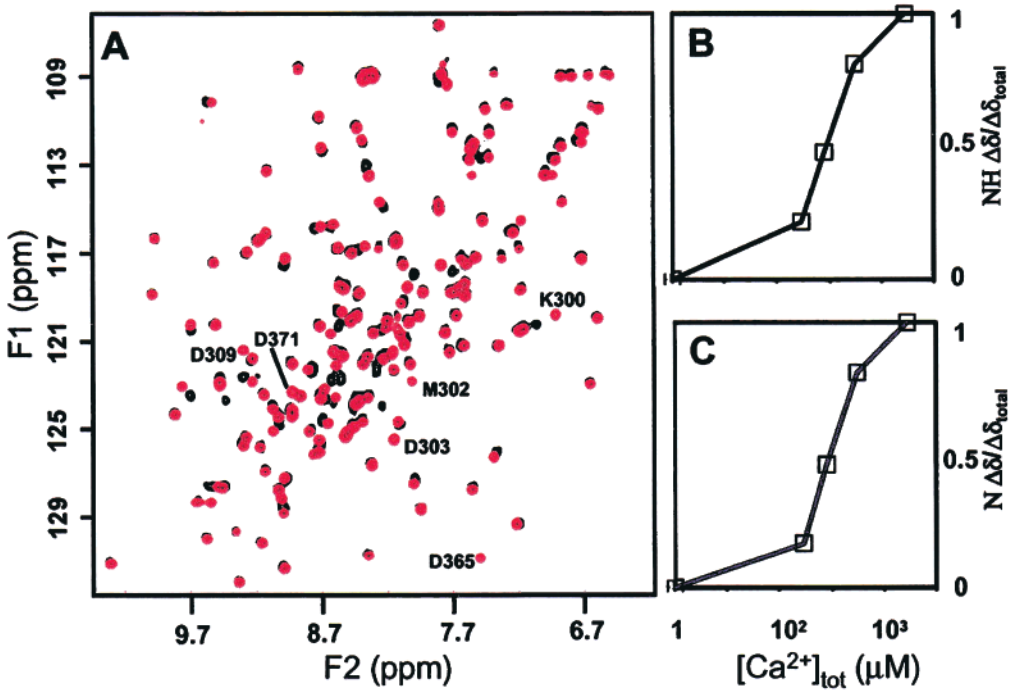

FIGURE 4: The synaptotagmin I C_2B domain is a functional Ca^{2+}-binding domain. (A) Superposition of ^{1}H−^{15}N HSQC spectra of the C_2B domain (0.1 mM) under analogous conditions to those described in Figure 3 with 1 mM EDTA (black contours) or 20 mM Ca^{2+} (red contours). Some of the cross-peaks that exhibit the largest Ca^{2+}-induced shifts are labeled next to their position in the Ca^{2+}-bound spectrum.[2] (B, C) Plots illustrating the Ca^{2+} dependence of the NH (B) and ^{15}N (C) chemical shifts of the K300 NH group. The chemical shift changes with respect to the Ca^{2+}-free form ($\Delta\delta$) were normalized with the total chemical shift change upon Ca^{2+} saturation ($\Delta\delta_{total}$).

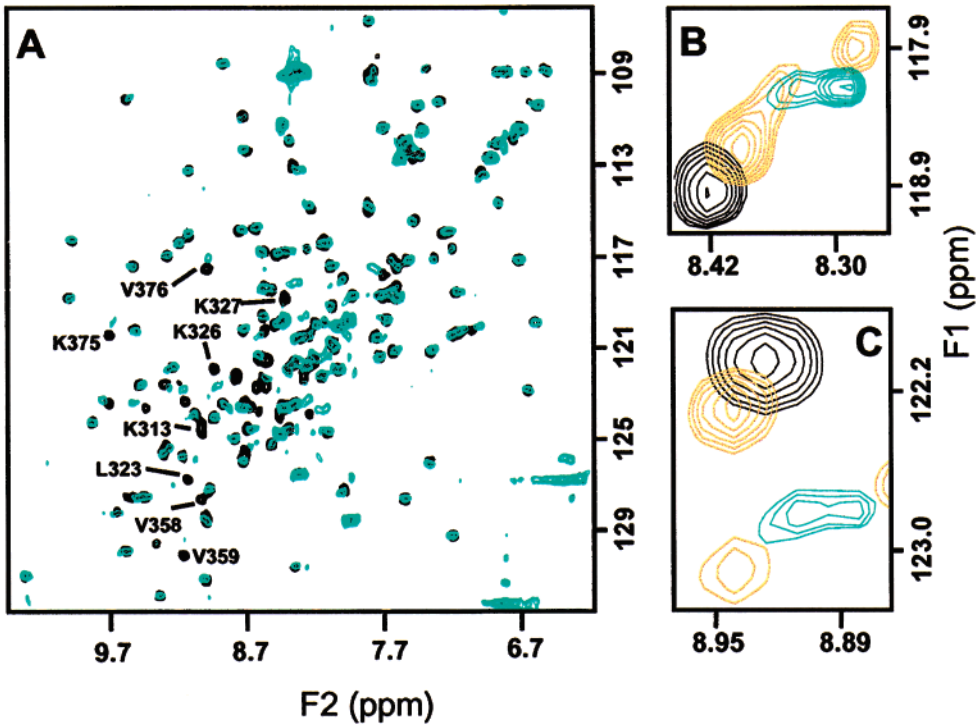

FIGURE 5: A polybasic region is involved in tight binding of nonproteinic contaminants to the C_2B domain. (A) Superposition of $^1H-^{15}N$ HSQC spectra (same conditions of Figure 3 with 1 mM EDTA) of 0.1 mM pure C_2B domain (black contours) and a 0.04 mM C_2B domain sample obtained after thrombin cleavage of a GST−C_2B domain fusion immobilized and washed by standard procedures (cyan contours). Some of the cross-peaks exhibiting shifts due to the contaminants are labeled. All residues exhibiting shifts are comprised within the K313−H315, R322−K327, V358−L362, and I373−V376 sequences, which are located at the concave side of the β-sandwich and are colored in blue or cyan in Figure 1C. (B, C) Expansions of the spectra shown in (A) corresponding to the regions containing the K327 (B) and K326 (C) cross-peaks. Also superimposed are the same regions of the $^1H-^{15}N$ HSQC spectrum of a 0.1 mM C_2B domain sample that was only purified by gel filtration in 0.2 M phosphate, pH 6.3, and 0.3 M NaCl (orange contours).

presence of 20 mM Ca^{2+} without significant resonance broadening. The line widths measured for well-resolved NH, aromatic, and methyl resonances are <16 Hz, consistent with a monomer but incompatible with a dimer. These results demonstrate that the C_2B domain does not directly dimerize as a function of Ca^{2+} even at high protein and Ca^{2+} concentrations. In agreement with this conclusion, no Ca^{2+}-induced increase in the apparent molecular weight of the C_2B domain was observed by gel filtration (data not shown). Parallel experiments with a fragment corresponding to the double C_2 domain region of synaptotagmin I (residues 140−421), purified by methods similar to those described for the C_2B domain, yielded analogous results with the expected increase in the line widths observed in the NMR spectra due to the higher molecular weight (data not shown). These data support previous analytical ultracentrifugation studies of the C_2B domain and the double C_2 domain region (*24*) and contradict GST pulldown experiments performed with recombinant proteins that suggested a direct Ca^{2+}-dependent dimerization of the C_2B domain (*21*).

A Polylysine Sequence Implicated in Protein−Protein Interactions Contains Stoichiometrically Bound Bacterial Contaminants. The presence of contaminants in GST−C_2B domain fusion proteins and their natural variability are likely sources for the numerous contradictory results obtained in studies of the C_2B domain binding activities. To analyze whether the contaminants bind to a particular region of the C_2B domain, we took advantage of the high sensitivity of $^1H-^{15}N$ HSQC spectra to binding interactions. Figure 5A shows a superposition of the $^1H-^{15}N$ spectrum of the pure C_2B domain (black contours) with that of a sample obtained after thrombin cleavage (cyan contours). The latter exhibits cross-peaks in the lower right corner that correspond to NH groups from basic side chains that are tightly bound to the contaminants. Note that these NH groups are usually not observable due to fast exchange with the solvent and do not appear in the spectrum of the pure C_2B domain. Figure 5A also shows that the backbone cross-peaks from a subset of residues are significantly shifted in the impure sample compared to the pure C_2B domain. Indeed, cross-peak multiplicity was observed for this subset of residues in impure samples, while only one cross-peak per residue is observed for the pure C_2B domain as expected for a homogeneous sample. This is illustrated for the cross-peaks of Lys326 and Lys327 in the expansions of Figure 5B,C, where the same spectra of Figure 5A are superimposed with an additional $^1H-^{15}N$ HSQC spectrum from a sample that was only purified by gel filtration (orange contours). Using the structure of the homologous rabphilin C_2B domain (*9*) as a model, all of the residues of the synaptotagmin I C_2B domain exhibiting cross-peak shifts in impure samples correspond to a polybasic region encompassing strand 4 and the preceding loop, as well as adjacent residues in the concave side of the β-sandwich (Figure 1C). These results show that, even after purification of GST−C_2B domain

[2] Details on the resonance assignment, structure determination, and Ca^{2+}-binding mode of the synaptotagmin I C_2B domain will be reported elsewhere (I. Fernandez et al., manuscript in preparation).

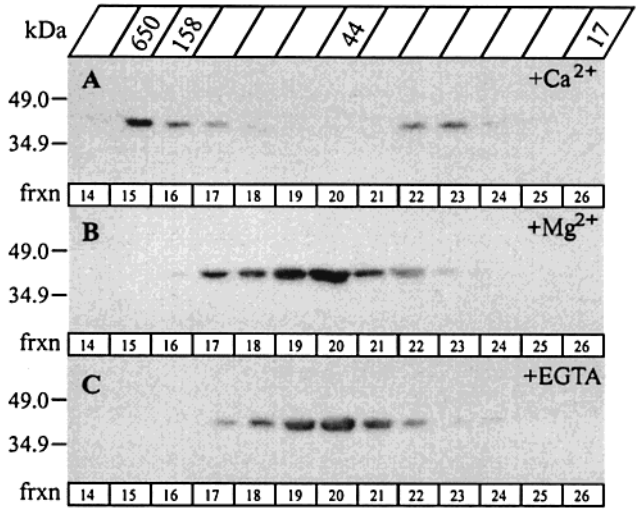

FIGURE 6: The cytoplasmic region of native synaptotagmin I assembles into a large complex as a function of Ca^{2+}. The soluble portion of trypsinized whole rat brain homogenate was applied to a gel filtration column, and 3 mL fractions were analyzed by SDS−PAGE followed by immunoblot using ECL detection. Blots of fractions 14−26 are shown for elutions performed in 100 mM NaCl in the presence of 2.5 mM Ca^{2+} (A), 2.5 mM Mg^{2+} (B), and 2.5 mM EGTA (C). Molecular weight standards for gel filtration and SDS−PAGE are indicated on the top and the left, respectively. The observation of a small amount of synaptotagmin fragment that elutes at low molecular weight in (A) is likely due to binding to the solid matrix in the presence of Ca^{2+}, which we have also observed for the recombinant synaptotagmin I double C_2 domain.

fusion proteins on affinity resins, this region of the synaptotagmin I C2B domain contains multiple tightly bound contaminants that most likely are polyacidic, such as nucleic acids. This is the same region that was implicated in Ca^{2+}-dependent dimerization of the C_2B domain and in its Ca^{2+}-independent interactions with AP-2 and Ca^{2+} channels by GST pulldown assays; these three interactions were disrupted by mutation of Lys326 and Lys327 to Ala (*16*). It is thus unclear whether these interactions directly involve the C_2B domain or are mediated by polyacidic contaminants.

Ca^{2+} Induces the Incorporation of Native Synaptotagmin I into a Large Complex. Since the recombinant GST−C_2B domain fusions that we and others had previously used to demonstrate the Ca^{2+}-dependent self-association of synaptotagmin I most likely contained bacterial contaminants, the immediate question that arises is whether Ca^{2+} can indeed cause multimerization of the native synaptotagmin I cytoplasmic region. To shed light on this question, we made use of the hypersensitive proteolytic site at residue 111 of synaptotagmin I (*10*, *11*). After mild trypsinolysis of whole rat brain homogenates and high-speed centrifugation, we analyzed the soluble fraction by gel filtration chromatography. The native synaptotagmin I fragment eluted as a monomer in the presence of 2.5 mM Mg^{2+} or 2.5 mM EGTA but appeared mostly in the void volume in the presence of 2.5 mM Ca^{2+} (Figure 6). These results show that the cytoplasmic region of native synaptotagmin I from brain homogenates assembles into a large complex as a function of Ca^{2+}. Since the recombinant synaptotagmin I C_2B domain or double C_2 domain region do not self-associate, assembly of this large complex either requires ternary components or involves posttranslational modification.

DISCUSSION

Synaptotagmin I is essential for fast Ca^{2+}-triggered neurotransmitter release, and strong evidence supports a role as a Ca^{2+} sensor in this process (*3*, *4*). The two C_2 domains of synaptotagmin I form most of its cytoplasmic region and are thus widely believed to constitute the business end of the molecule. Characterizing the interactions of the C_2 domains is thus critical to understand how synaptotagmin I may be involved in Ca^{2+} triggering of neurotransmitter release, but studies of the C_2B domain had yielded a number of confusing results. The results described here have several implications for the potential roles of the synaptotagmin I C_2B domain and provide plausible explanations for some of these confusing results.

First, we show that the C_2B domain is a functional Ca^{2+}-binding domain that can cooperate with the C_2A domain in the Ca^{2+}-sensing function of synaptotagmin I. Second, we show that the recombinant C_2B domain is not capable of Ca^{2+}-dependent homodimerization. Thus, while we find that Ca^{2+} causes incorporation of the native synaptotagmin I cytoplasmic region into a large complex that could be involved in formation of the fusion pore, direct self-association of the C_2B domain can only be involved in this complex via posttranslational modification. Finally, we uncovered the presence of tightly bound bacterial contaminants in the recombinant GST−C_2B domain, attached to a specific polybasic sequence that had been implicated in multiple interactions. This finding injects an element of caution in interpreting GST pulldown experiments performed with GST fusions that are only isolated by affinity chromatography. Even in cases where soluble recombinant proteins are further purified, biophysical characterization is desirable to ensure their purity and proper folding. In the case of the C_2B domain, the tightly bound polyacidic contaminants may have promoted irrelevant interactions while inhibiting biologically significant activities. At the same time, the variability of the contaminants (and probably in the purification methods used) provides a likely explanation for the numerous contradictory results obtained in studies of the C_2B domain. Contradictions may have also arisen in some cases from a mutation in the C_2B domain sequence (Gly374→Asp), which in our hands hinders proper folding of the domain.

In view of these results, previous studies of the interactions of the synaptotagmin I C_2B domain by our laboratory and others need to be reevaluated. Clearly, the polybasic region of the C_2B domain is very reactive. Clarifying which are the relevant interactions of this region and which are the Ca^{2+}-dependent targets of the C_2B domain will be critical to understand the mechanism of action of synaptotagmin I. It will also be crucial to unravel the composition of the large complex that includes the Ca^{2+}-bound synaptotagmin I cytoplasmic fragment and the interactions that mediate its assembly.

REFERENCES

1. Südhof, T. C., and Rizo, J. (1996) *Neuron 3*, 379−388.
2. Marquèze, B., Berton, F., and Seagar, M. (2000) *Biochimie 82*, 409−420.
3. Geppert, M., Goda, Y., Hammer, R. E., Li, C., Rosahl, T. W., Stevens, C. F., and Südhof, T. C (1994) *Cell 79*, 717−727.
4. Fernández-Chacón, R., Königstorfer, A., Gerber, S. H., Garcia, J., Matos, M. F., Stevens, C. F., Brose, N., Rizo, J., Rosenmund, C., and Südhof, T. C. (2001) *Nature 410*, 41−49.

5. Bennett, M. R. (1999) *Prog. Neurobiol. 59*, 243−277.
6. Sutton, R. B., Davletov, B. A., Berghuis, A. M., Südhof, T. C., and Sprang, S. R. (1995) *Cell 80*, 929−38.
7. Shao, X., Fernandez, I., Südhof, T. C., and Rizo, J. (1998) *Biochemistry 37*, 16106−16115.
8. Ubach, J., Zhang, X., Shao, X., Südhof, T. C., and Rizo, J. (1998) *EMBO J. 17*, 3921−3930.
9. Ubach, J., Garcia, J., Nittler, M. P., Südhof, T. C., and Rizo, J. (1999) *Nat. Cell Biol. 1*, 106−112.
10. Perin, M. S., Brose, N., Jahn, R., and Südhof, T. C (1991) *J. Biol. Chem. 266*, 623−629.
11. Brose, N., Petrenko, A. G., Südhof, T. C., and Jahn, R (1992) *Science 256*, 1021−1025.
12. von Poser, C., Zhang, J. Z., Mineo, C., Ding, W., Ying, Y., Südhof, T. C., and Anderson, R. G. (2000) *J. Biol. Chem. 275*, 30916−30924.
13. Bai, J., Earles, C. A., Lewis, J. L., and Chapman, E. R. (2000) *J. Biol. Chem. 275*, 25427−25435.
14. Sugita, S., Hata, Y., Südhof, T. C (1996) *J. Biol. Chem. 271*, 1262−1265.
15. Chapman, E. R., An, S., Edwardson, J. M., and Jahn, R. (1996) *J. Biol. Chem. 271*, 5844−5849.
16. Chapman, E. R., Desai, R. C., Davis, A. F., and Tornehl, C. K. (1998) *J. Biol. Chem. 273*, 32966−32972.
17. Osborne, S. L., Herreros, J., Bastiaens, P. I., and Schiavo, G. (1999) *J. Biol. Chem. 274*, 59−66.
18. Littleton, J. T., Serano, T. L., Rubin, G. M., Ganetzky, B., and Chapman, E. R. (1999) *Nature 400*, 757−760.
19. Thomas, D. M., Ferguson, G. D., Herschman, H. R., and Elferink, L. A. (1999) *Mol. Biol. Cell 10*, 2285−2295.
20. Fukuda, M., Kanno, E., and Mikoshiba, K. (1999) *J. Biol. Chem. 274*, 31421−3147.
21. Desai, R. C., Vyas, B., Earles, C. A., Littleton, J. T., Kowalchyck, J. A., Martin, T. F., and Chapman, E. R. (2000) *J Cell Biol. 150*, 1125−1136.
22. Fukuda, M., and Mikoshiba, K. (2000) *J. Biol. Chem. 275*, 28180−28185.
23. Butz, S., Fernandez-Chacon, R., Schmitz, F., Jahn, R., and Südhof, T. C. (1999) *J. Biol. Chem. 274*, 18290−18296.
24. Garcia, R. A., Forde, C. E., and Godwin, H. A. (2000) *Proc. Natl. Acad. Sci. U.S.A. 97*, 5883−5888.
25. Zhang, J. Z., Davletov, B. A., Südhof, T. C., and Anderson, R. G. (1994) *Cell 78*, 751−760.
26. Sheng, Z.-H., Yokoyama, C. T., and Catterall, W. A. (1997) *Proc. Natl. Acad. Sci. U.S.A. 94*, 5405−5410.
27. Fukuda, M., Aruga, J., Niinobe, M., Aimoto, S., and Mikoshiba, K. (1994) *J. Biol. Chem. 269*, 29206−29211.
28. Fukuda, M., Kojima, T., Aruga, J., Niinobe, M., and Mikoshiba, K. (1995) *J. Biol. Chem. 270*, 26523−26527.
29. Schiavo, G., Gmachl, M. J. S., Stenbeck, G., Söllner, T. H., and Rothman, J. E. (1995) *Nature 378*, 733−736.
30. Schivell, A. E., Batchelor, R. H., and Bajjalieh, S. M (1996) *J. Biol. Chem. 271*, 27770−27775.
31. Guan, K. L., and Dixon, J. E. (1991) *Anal. Biochem. 192*, 262−267.
32. Zhang, O., Kay, L. E., Olivier, J. P., and Forman-Kay, J. (1994) *J. Biomol. NMR 4*, 845−858.
33. Perin, M. S., Fried, V. A., Mignery, G. A., Jahn, R., and Südhof, T. C. (1990) *Nature 345*, 260−263.
34. Perin, M. S., Johnston, P. A., Ozcelik, T., Jahn, R., Francke, U., and Südhof, T. C. (1991) *J. Biol. Chem. 266*, 615−622.
35. Davletov, B., Sontag, J.-M., Hata, Y., Petrenko, A. G., Fykse, E. M., Jahn, R., and Südhof, T. C. (1993) *J. Biol. Chem. 268*, 6816−6822.
36. Nalefsky, E. A., and Falcke (1996) *Protein Sci. 5*, 2375−2390.
37. Shao, X., Davletov, B. A., Sutton, R. B., Südhof, T. C., and Rizo, J. (1996) *Science 273*, 248−251.
38. Zhang, X., Rizo, J., and Südhof, T. C. (1998) *Biochemistry 37*, 12395−12403.
39. Koradi, R., Billeter, M., and Wüthrich, K. (1996) *J. Mol. Graphics 14*, 51−55.

BI010340C